SHOCK STRUCTURE AND ITS EFFECT ON ELECTRON ACCELERATION IN QUASI-PERPENDICULAR SHOCKS

R. E. Lowe[1], **D. Burgess**[1]

[1]Astronomy Unit, Queen Mary and Westfield College,
Mile End Road, London E1 4NS, United Kingdom
(fax: +44 20 8983 3522; email: R.Lowe@qmw.ac.uk)

ABSTRACT

Highly energetic electrons near collisionless shocks are widely observed, but the exact electron acceleration mechanism is not completely understood. Simulations of quasi-perpendicular collisionless shocks show ripples in the density and magnetic field moving along the shock ramp. Using a two dimensional hybrid simulation and a test particle code, we examine these ripples and their effect on electron acceleration.

Key words: electron acceleration; collisionless shocks.

1. INTRODUCTION

Adiabatic reflection provides a mechanism for accelerating electrons at a quasi-perpendicular shock. The change in velocity is limited by the de Hoffmann-Teller velocity [Leroy & Mangeney 1984; Wu 1984]. Observations downstream of the Earth's bow shock by Gosling et al. (1989) reveal a population of electrons which exhibit an energy distribution with a power law tail extending as far as 20 keV. One dimensional simulations show that such populations are too energetic to be explained by adiabatic reflection unless the shock is almost exactly perpendicular [Krauss-Varban et al. 1989]. We examine how two dimensional structure, in the form of ripples on the shock surface, can affect electron behaviour. This is done by taking the time varying fields from a self consistent shock simulation and using them in a test particle simulation of superthermal electron motion.

In our simulations, ripples are ion scale features at the shock front, which are seen to move along the overshoot. They are most clearly visible in the shock normal component of the magnetic field (Figure 1). A strictly one dimensional shock has a constant normal magnetic field component, so there is little in the way of additional magnetic structure. Indirect observational evidence for ripples comes from measurements of whistler waves upstream of collisionless shocks [Orlowski et al. 1995].

The process that generates the ripples remains poorly

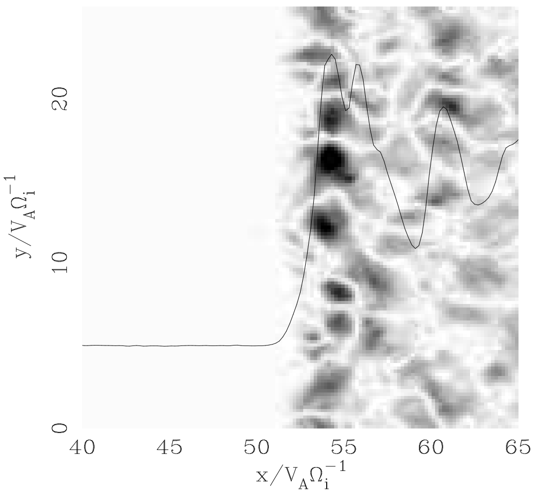

Figure 1. Map of B_x with $|\mathbf{B}|$ profile superimposed. B_x maximum $= 2B_0$, $\theta_{B_n} = 88°$, inflow $= 4V_A$

understood. One possible mechanism is an instability driven by reflected ions gyrating back into the shock [McKean et al. 1995]. Ripples could also be caused by wave trapping at the front due to the variation of the Alfvén speed through the shock ramp and overshoot. Work is currently in progress to study this latter possibility.

2. SHOCK FRONT RIPPLES

2.1. Hybrid Code

We have used a hybrid code (ion macroparticles and an inertialess electron fluid) as described by Matthews (1994). The code is self-consistent and our implementation is 2-D in space and 3-D in velocity.

The choice of a hybrid code means that electron physics is not well modelled. In the context of shocks, this means that we do not see some effects that occur in full particle simulations, such as electron scale ripples, but we do observe ion scale ripples, which are generally too large to be modelled by existing full particle PIC codes. Because of their high speed,

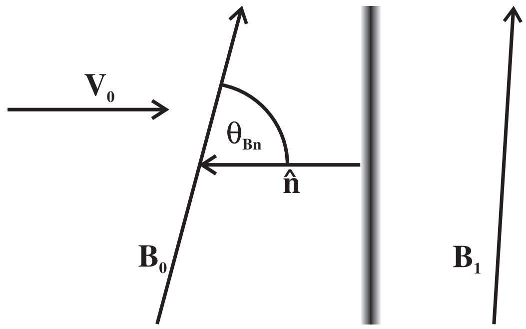

Figure 2. Shock geometry

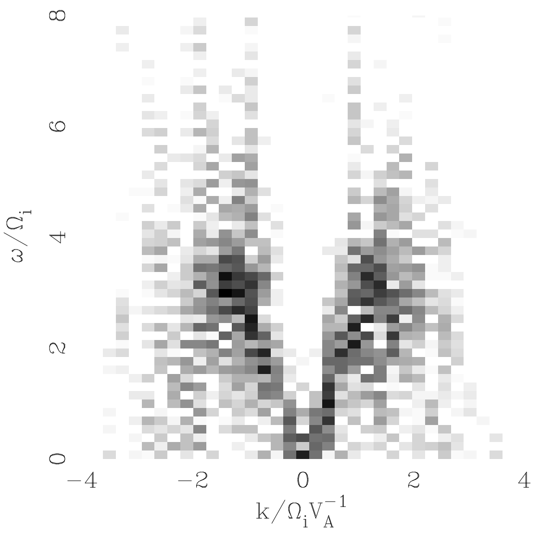

Figure 3. A Fourier Transform of B_x slices showing the ripples' dispersion relation. The normalizations use upstream values.

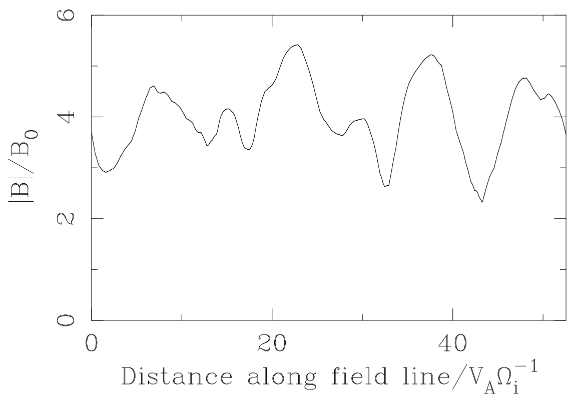

Figure 4. The variation of $|\mathbf{B}|$ along a field line running along the shock front.

electrons travel many ion inertial lengths along the shock as they interact with the shock. Thus they will feel the effects of ion scale fluctuations.

Our simulation is set up as shown in Figure 2. We generate a shock by reflecting homogeneous plasma, moving at constant velocity, off a stationary perfectly conducting barrier. We use an electron plasma beta $\beta_e = 0.5$. This is a standard method for launching a shock, which is physically simple, but provides a clean shock once the shock front is clear of the reflecting barrier. This configuration has limitations: the shock is planar, so we are neglecting curvature effects [Krauss-Varban & Burgess 1991]; the upstream plasma is smooth, so we are neglecting upstream waves and bulk inhomogeneity; and there is a barrier downstream, which prevents us from modelling wave sources there.

We conduct simulations using two orientations of the upstream magnetic field, $\mathbf{B}_0$. The first has $\mathbf{B}_0$ lying in the plane of the simulation, allowing electrons to move along the field line and feel the full 2-D field structure. The second has $\mathbf{B}_0$ pointing out of the simulation plane, so that the electrons feel little variation along the field line. This is intended to mimic a 1-D simulation.

2.2. Ripple properties

The strength of ripples increases with both the Alfvén Mach number, M_A, and the angle between the upstream magnetic field and the shock normal, θ_{B_n}.

We take slices transverse to the shock of the normal component of the magnetic field at successive time steps and Fourier Transform to obtain an $\omega - k$ diagram (Figure 3). By comparing dispersion relations at $\theta_{B_n} = 85°$ with different inflow velocities, we find that the speed of the shock front ripples along the shock front is the same as the downstream Alfvén speed.

Adiabatic reflection requires us to assume that the shock structure is stationary, one-dimensional and that the electron gyroradius is much smaller than the shock thickness. In our simulations with $\mathbf{B}_0$ in the simulation plane, these approximations are violated: we observe magnetic structures that are time dependent and cannot be approximated as one-dimensional. Figure 3 also shows power over a range of ω and k, which could lead to electron scattering.

As can be seen from Figure 1, the ripples have a wavelength of a few ion inertial lengths, which corresponds to the region of maximum power in Figure 3. The amplitude of the peaks in B_x is around $2B_0$. These peaks also appear to be connected to structure behind the shock. The variation in the magnetic field along a field line passing through the shock front suggests the possibly of magnetic mirroring (Figure 4). Since the structure is time dependent, there also exists the possibility of First Order Fermi acceleration [Gisler & Lemons 1990].

3. ELECTRON ACCELERATION

3.1. Adiabatic Reflection

The fraction of incoming electrons reflected depends on the maximum value of the magnetic field, B_1, at the shock overshoot [Leroy & Mangeney 1984; Wu 1984]. In order to compare simulation results with predictions from adiabatic theory, we describe a simplified geometry in which the upstream flow is parallel to the shock normal in the simulation and shock frames (Figure 2).

Adiabatic theory is applied in the de Hoffmann-Teller frame. This means that the motional electric field ($-\mathbf{V}\times\mathbf{B}$) is zero and we can consider an electron to conserve its energy. The velocity required to transform to this frame from the shock frame is:

$$\mathbf{V}_{\rm HT} = \frac{\hat{\mathbf{n}}\times(\mathbf{V}_0\times\mathbf{B}_0)}{\mathbf{B}_0\cdot\hat{\mathbf{n}}} \tag{1}$$

where $\mathbf{V}_0$ is the upstream flow velocity. In the geometry of the simulation, this gives:

$$\mathbf{V}_{\rm HT}\cdot\hat{\mathbf{B}}_0 = \frac{-V_0\sin^2\theta_{\rm B_n}}{\cos\theta_{\rm B_n}} \tag{2}$$

We shall denote quantities in the de Hoffmann-Teller frame with a tilde and unit vectors with a hat. We transform the components, perpendicular and parallel to $\mathbf{B}_0$, of an electron's velocity in the upstream plasma rest frame, $\mathbf{v}$:

$$\tilde{v}_{\|} = v_{\|} - (\mathbf{V}_{\rm HT}-\mathbf{V}_0)\cdot\hat{\mathbf{B}}_0 \tag{3}$$

$$\tilde{v}_{\perp} = v_{\perp} \tag{4}$$

In adiabatic theory, we assume the conservation of perpendicular magnetic moment, μ. The velocity components in the reflected distribution are:

$$v_{\|\rm r} = -v_{\|} + 2(\mathbf{V}_{\rm HT}-\mathbf{V}_0)\cdot\hat{\mathbf{B}}_0 \tag{5}$$

$$v_{\perp\rm r} = v_{\perp} \tag{6}$$

We shall express velocity components in terms of the pitch angle, α:

$$v_{\|} = v\cos\alpha \tag{7}$$

$$v_{\perp} = v\sin\alpha \tag{8}$$

In our simulations, the initial electron test particle distribution consists of a uniformly covered spherical shell in velocity space. We can calculate the fraction of reflected ions by finding the values of α between which reflection occurs:

$$\frac{F_{\rm r}}{F_{\rm tot}} = \frac{\cos\alpha_{\rm min}-\cos\alpha_{\rm max}}{2} \tag{9}$$

There are two processes that constrain these angles. The first is the conservation of magnetic moment. Magnetic reflection will occur if and only if the electron cannot conserve its magnetic moment while crossing the shock. If the potential difference between the upstream and the overshoot is ϕ_0, then the condition for reflection is:

$$\mu \geq \frac{e\tilde{\phi_0}+\frac{1}{2}m\tilde{v}^2}{B_1} \tag{10}$$

This leads to a constraint on α, which must be between the two solutions of

$$a\cos^2\alpha + b\cos\alpha + c = 0 \tag{11}$$

$$a = \frac{B_1}{B_0} \tag{12}$$

$$b = \frac{(\mathbf{V}_{\rm HT}-\mathbf{V}_0)\cdot\hat{\mathbf{B}}_0}{v} \tag{13}$$

$$c = \frac{e\tilde{\phi_0}}{\frac{1}{2}mv^2} + \left(\frac{(\mathbf{V}_{\rm HT}-\mathbf{V}_0)\cdot\hat{\mathbf{B}}_0}{v}\right)^2 - \frac{B_1-B_0}{B_0} \tag{14}$$

In order for a reflected electron to escape upstream, it must travel along the upstream field with sufficient speed to overcome the flow of plasma into the shock. This introduces a cut-off parallel velocity to the reflected component of the distribution that depends strongly on $\theta_{\rm B_n}$. This introduces the second constraint on α:

$$\cos\alpha \geq \frac{V_0}{v\cos\theta_{\rm B_n}} + 2\frac{(\mathbf{V}_{\rm HT}-\mathbf{V}_0)\cdot\hat{\mathbf{B}}_0}{v} \tag{15}$$

There may be a fraction of the initial electron distribution that escapes upstream without interacting with the shock. We disregard this population and modify the value of $F_{\rm tot}$ accordingly.

We can calculate the energy spectrum, $f(E)$, in the upstream plasma frame. There are two populations. The first, transmitted, population is accelerated only by the cross-shock potential, ϕ:

$$f(E) = \delta(E; e\tilde{\phi} + \frac{1}{2}mv^2)\frac{F_{\rm tot}-F_{\rm r}}{F_{\rm tot}} \tag{16}$$

The second, reflected, population has a flat spectrum between two energies, $E_{\rm max}$ and $E_{\rm min}$, which are determined by applying Equations 5 and 6 to the critial angles $\alpha_{\rm min}$ and $\alpha_{\rm max}$:

$$f(E) = \frac{1}{E_{\rm max}-E_{\rm min}}\frac{F_{\rm r}}{F_{\rm tot}} \tag{17}$$

for $E_{\rm min} \leq E \leq E_{\rm max}$ and $f(E) = 0$ otherwise.

3.2. Simulation Parameters

We investigate electron behaviour by following the trajectories of test particles. We follow Krauss-Varban et al. (1989) by using a high order integration scheme. Our implementation of the code is relativistic and, in tests, conserves both energy and perpendicular magnetic moment well. We used an Alfvén speed $V_{\rm A} = 60$ km/s and an inflow velocity of $4V_{\rm A}$ in the simulation frame, giving a shock with $V_0 \approx 5.7V_{\rm A}$. These parameters were chosen to resemble conditions in the Earth's bow shock. Shock properties are a strong function of $\theta_{\rm B_n}$. We study two cases: $\theta_{\rm B_n} = 85°$ and $\theta_{\rm B_n} = 88°$. This gives us four combinations of simulation parameters.

The electrons were released with a common gyrocentre at an energy of 100 eV, corresponding to the tail of the solar wind halo distribution. In velocity space, the initial electron distribution is a uniformly covered spherical shell with a cut-off corresponding to electrons that escape upstream without interacting with the shock.

In our simulations, we measured an overshoot magnetic field, B_1, in the range $5.1B_0$ to $5.5B_0$. In the following calculations, we have assumed a value of $B_1 = 5.2B_0$. We follow Krauss-Varban et al. (1989) by assuming a canonical value of 85 eV for the potential difference between the upstream and the overshoot. Using these values, we can use adiabatic theory to predict properties of the final electron distributions (Tables 1 and 2).

3.3. Energy Spectra

Energy spectra are shown for the upstream and downstream distributions in Figure 5. Comparisons with predicted parameters from adiabatic theory are given in Tables 1 and 2. We observe electron distributions that are broadly consistent with adiabatic theory when $\mathbf{B}_0$ is directed out of the simulation plane, when there is little variation of $\mathbf{B}$ along the field lines. The distributions when $\mathbf{B}_0$ is in the simulation plane, however, differ. This indicates that two-dimensional structure does affect electron behaviour. We also note that the fraction of reflected electrons at $\theta_{\mathrm{B_n}} = 88°$ is reduced by a factor of ~ 10 in comparison to the predictions of adiabatic theory.

Observations downstream of the Earth's bow shock by Gosling et al. (1989) reveal a population of electrons at significantly higher energies than can be produced by simple application of adiabatic theory. They report a power law distribution of velocities taking the form:

$$f(v) \sim E^{-3.7} \tag{18}$$

It is interesting to note that our simulations produce spectra which are consistent with a power law when $\mathbf{B}_0$ is directed in the plane of the simulation. We do not, however, expect to reproduce the observed power law index, since our initial electron distribution function does not mimic the full solar wind distribution.

It is also significant that the upstream and downstream distributions are similar when $\mathbf{B}_0$ is in the simulation plane and electrons are allowed to feel the spatial variations in the magnetic field. This suggests that reflections occur within the shock to such an extent that the two distributions become mixed and therefore similar, apart from the upstream cut-off imposed by the shock geometry.

4. CONCLUSIONS

Two dimensional hybrid simulations of quasi-perpendicular shocks show ripples in the fields that move along the shock front at the downstream Alfvén speed.

We have shown that the accelerated electron distribution function depends on whether the upstream magnetic field is in, or out of, the plane of the simulation, suggesting that 2-D structure is important in understanding the acceleration process. When 2-D structure is included, the upstream and downstream populations are similar at energies above a cut-off that is determined by the shock geometry. This suggests that there is additional scattering, which can be attributed to the 2-D structure.

In future, we hope to improve the electron test particle code by the use of cubic spline interpolation for the fields. We also propose to study the effect of downstream waves on ripple formation by artificially damping downstream wave activity.

An obvious criticism of this kind of study is the tight restriction placed on $\theta_{\mathrm{B_n}}$ required to produce appreciable rippling. We propose to consider the effects of both large and small scale inhomogeneities in the upstream field. Large scale effects will be examined by adding a bend to the upstream field. Small scale deviations can be studied by introducing upstream waves. The addition of such inhomogeneities will more accurately resemble the conditions seen at actual shocks and may increase the range of $\theta_{\mathrm{B_n}}$ over which ripples are significant.

ACKNOWLEDGMENTS

This work was supported by a PPARC (UK) studentship and by PPARC grant GR/L39094.

REFERENCES

Gisler, G., Lemons, D. 1990, J. Geophys. Res., 95, 14925

Gosling, J.T., Thomsen, M.F., Bame, S.J., Russell, C.T., 1989, J. Geophys. Res., 94, 10011

Hellinger, P., Mangeney, A., Matthews, A., 1996, Geophys. Res. Lett., 95, 14925

Krauss-Varban, D., Burgess, D., Wu, C.S., 1989, J. Geophys. Res., 94, 15089

Krauss-Varban, D., Burgess, D., 1991, J. Geophys. Res., 96, 143

Leroy, M.M., Mangeney, A. 1984, Annales Geophys., 2, 449

McKean, M.E., Omidi, N., Krauss-Varban, D., 1995, J. Geophys. Res., 100, 3427

Matthews, A. 1994, J. Comput. Phys., 112, 102

Orlowski, D.S., Russel, C.T., Wu, C.S., Krauss-Varban, D., Omidi, N., Thomsen, M.F., 1995, J. Geophys. Res., 100, 17117

Wu, C.S. 1984, J. Geophys. Res., 89, 8857

Parameters	Upstream	Downstream	In Shock
$\theta_{\mathrm{B_n}} = 85°$, adiabatic	87%	13%	-
$\theta_{\mathrm{B_n}} = 85°$, $\mathbf{B}_0$ out of plane	73.9%	23.4%	2.7%
$\theta_{\mathrm{B_n}} = 85°$, $\mathbf{B}_0$ in plane	46.8%	51.7%	1.5%
$\theta_{\mathrm{B_n}} = 88°$, adiabatic	33%	67%	-
$\theta_{\mathrm{B_n}} = 88°$, $\mathbf{B}_0$ out of plane	27.2%	71.6%	1.2%
$\theta_{\mathrm{B_n}} = 88°$, $\mathbf{B}_0$ in plane	3.2%	96.7%	0.1%

Table 1. The location of particles at the end of the simulation, compared with predictions made through adiabatic theory.

Parameters	α_{min}	α_{max}	E_{min}	E_{max}
$\theta_{\mathrm{B_n}} = 85°$	36°	131°	0.15 keV	0.39 keV
$\theta_{\mathrm{B_n}} = 88°$	60°	100°	0.99 keV	1.37 keV

Table 2. Electron distribution function parameters as derived from adiabatic theory.

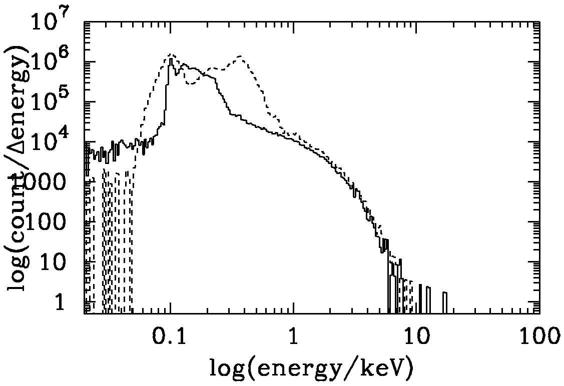

(a) $\theta_{\mathrm{B_n}} = 85°$, $\mathbf{B}_0$ out of plane

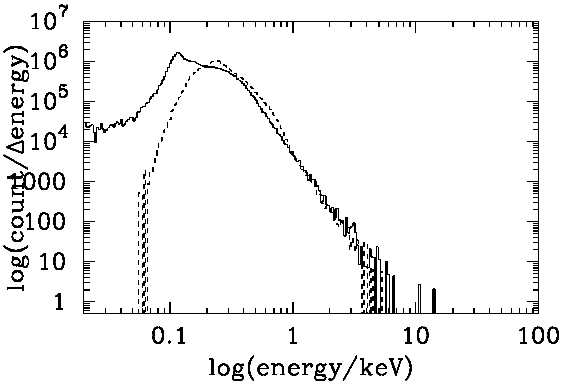

(b) $\theta_{\mathrm{B_n}} = 85°$, $\mathbf{B}_0$ in plane

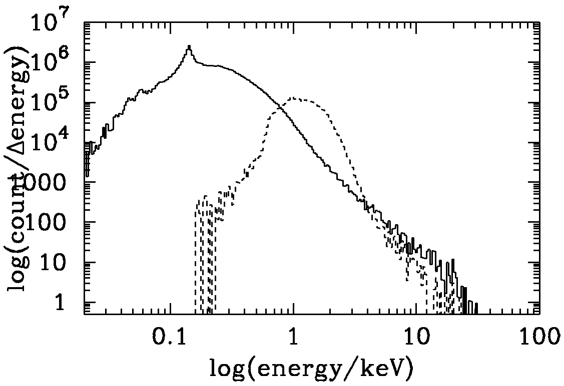

(c) $\theta_{\mathrm{B_n}} = 88°$, $\mathbf{B}_0$ out of plane

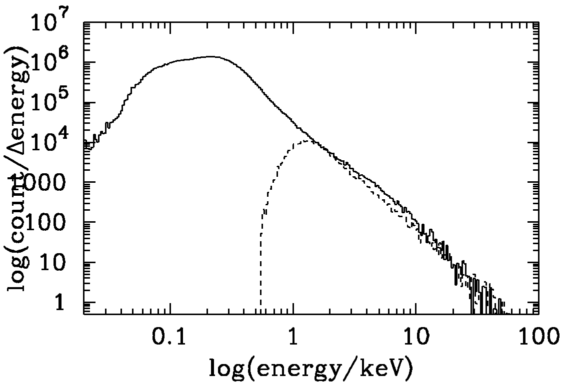

(d) $\theta_{\mathrm{B_n}} = 88°$, $\mathbf{B}_0$ in plane

Figure 5. Electron logarithmic energy spectra. The downstream population is represented by solid lines and the upstream population by dashed lines. The energies are calculated in the upstream plasma frame.